



## Optimised hydrodynamics for membrane bioreactors with immersed flat sheet membrane modules

H. Prieske<sup>a,\*</sup>, L. Böhm<sup>a</sup>, A. Drews<sup>b</sup>, M. Kraume<sup>a</sup>

<sup>a</sup>Technische Universität Berlin, Chair of Chemical and Process Engineering, Straße des 17. Juni 135, 10623 Berlin, Germany  
email: h.prieske@mailbox.tu-berlin.de, matthias.kraume@tu-berlin.de

<sup>b</sup>University of Oxford, Dept. of Engineering Science, Parks Rd, Oxford OX1 3PJ, UK

Received 3 June 2009; Accepted 4 January 2010

### ABSTRACT

Since aeration is the largest cost factor in membrane bioreactor (MBR) operation it is clear that the biggest leap towards energy and operational costs savings can be achieved by improving the use of air. Many basics of the complex two-phase flow in membrane modules and in the overall MBR tank as well as their interactions, however, are still poorly understood. This work focuses both on fundamental studies on shear stress exerted by rising bubbles and on optimising the geometries of tank and module accordingly in order to obtain an improved deposition control at minimum energy input. For both, parameter studies were carried out by numerical simulations which were validated with experimental measurements. The optimum bubble size/channel width combination depended on the superimposed liquid velocity. The relationship between the liquid circulation velocity and the aeration intensity was measured for different reactor and module geometries. A modification of the Chisti model for airlift loop reactors was also performed which can be used as a design rule for tank and module geometry or aeration rate. At the same gas flow rate, a 30–50% increase in liquid circulation velocity was achieved by a simple modification of the sparger and the entry zone to the riser section.

**Keywords:** Air scour; Fouling; Hydrodynamic optimisation; MBR design; Shear stress; Single bubble

### 1. Introduction

One of the main drawbacks of membrane bioreactors (MBRs) are the higher operational costs in comparison to conventional activated sludge plants. Especially the energy consumption for air scouring to limit the cake layer on the membranes still causes significantly higher costs with up to 60% of the total energy costs [1–3].

Gas sparging is an established method to limit depositions on membranes and often the subject of publications related to membrane processes [4].

More literature is available on gas/liquid flow inside tubular membranes [5] or around submerged hollow fibres [6–8]. Due to this and the fact that hydrodynamic parameters such as the bubble distribution are somewhat easier to control in flat sheet than in hollow fibre modules, this work will focus on the former. Since many fundamentals of multiphase flow in MBRs are still unknown and difficult to access experimentally, there is no common way to construct and operate flat sheet modules as yet (see Table 1) which leads to a wide range of specific aeration demand ( $SAD_m$ ) values and waste of energy.

\*Corresponding author.

Table 2 summarises the available literature on bubbles in flat sheet modules. Published investigations have a number of different shortcomings resulting from inevitable assumptions and simplifications made to enable experimental or numerical investigation of the complex and interacting system. Typically, set-up heights are too low to allow terminal bubble rise velocities to be reached. Calculations and experiments in the current work showed that a much longer rising path than, e.g., 147 mm [9,10,13] (Cabassud's group), is necessary for a single bubble to reach a steady state. 2D numerical inves-

tigations do not take into account any wall effects which are obviously very important in the studied system with a bubble of an equivalent diameter of 15.7 mm in a 5 mm gap [10]. Further, the influence of circulating flow which occurs in typical MBRs is frequently neglected when just investigating hydrodynamics inside a module [11,15]. Nagaoka et al. (2003) used a mechanical shear stress sensor but only tested a 32 mm gap which is unrepresentative of commercial modules (cf. Table 1) [12].

The aim of this work therefore is a systematic investigation of influencing geometrical and operational

Table 1  
Specifications of commercially available flat sheet modules.

Manufacturer / model	Membrane spacing (mm)	Panel height (mm)	SADm ( $\text{m}^3/(\text{m}^2\text{h})$ )	Superficial gas velocity (m/s)	Aeration
A3 Water Solutions / M70	7	1050	0.31	0.025	fine
Brightwater Eng. / Membright	9	950	1.28	0.076	coarse
Colloide Engineering Systems / Sub snake	10	1000	0.5	0.028	fine
Kubota Corporation / 510 ES (single-deck)	7	1000	0.75	0.047	coarse
Microdyn Nadir / BioCel BC100-50	8	1200	0.3 - 0.8	0.0125 - 0.033	fine
Toray Industries / TRM140-100S	6	1608	0.3	0.037	

Table 2  
Literature on bubbles in flat sheet modules.

Ref.	Add. liq. CF/downcomer zone	Set-up height (mm)	Membrane spacing (mm)	Method	System	Investigated parameters
Nagaoka et al. 2003 [12] (methyl cellulose)	yes	1000	32	exp.	air/water	
Essemiani et al. 2001 [10] (electrolyte)	yes	147	5	exp./num. (2D)	air/water	
Ducom et al. 2002, 2003 [9,13] (electrolyte)	yes	147	5	exp.	air/water	
Sofia et al. 2004 [14]	yes	400	n.a. (rather wide)	exp.	air/act. sludge	circulation velocity
Ndinisa et al. 2006a,b [11,15]	no	490	7–14	exp./num. (3D)	air/water	bubbles size, shear stress
Prieske et al. 2008 [16]	yes	1700	5–9	exp./num. (3D)	air/water	circulation velocity
Drews et al. 2008a,b [17,18]	yes	1700	3–11	exp./num. (3D)	air/water, air/act. sludge	rise velocity, shear stress, circ. vel.
Zhang et al. 2009 [19]	yes	1000	20	exp.	air/water	shear stress
This study	yes	1200/700	3–10	num. (3D)	air/water	rise velocity, shear stress

\*Not Available

parameters on fouling reduction by aeration of flat sheet membrane modules which enables subsequent optimisation. Besides aeration rate and bubble size (or diffuser ports), module and tank geometry (membrane spacing, liquid level, cross-sectional areas of riser and downcomer, etc.) have decisive effects on the achieved crossflow velocity, shear stress and bubble-membrane-contact. A systematic hydrodynamic investigation thus needs to take into account several fundamentals of this gas/liquid flow, starting from single bubble movement in submerged modules to gas/liquid motion in the whole tank.

## 2. Materials and Methods

### 2.1. Experimental methods

*Single bubble experiments.* The movement of single bubbles (equivalent spherical diameter: 3–24 mm) in stagnant water between two vertical plates (spacing: 3–11 mm, height: 700 mm, see Fig. 1) was recorded using a high-speed camera (MV-D752, Photonfocus AG). From this, the terminal rising velocity was determined which together with the observed bubble shape and path served as a validation for numerical simulations. At least 15 bubbles were recorded for each bubble size/spacing combination, and the standard deviation was less than 5%.

*Tank flow.* To determine the global flow pattern, a pseudo-2D membrane tank model with typical full scale dimensions was set up (see Fig. 1). To enable optical accessibility, the depth was only 0.1 m, assuming that despite this small depth the tank wall friction is negligible in comparison with losses caused by bends and

friction inside the module. The module was simulated by inserting acrylic plates (wall thickness 5 mm). The riser region was aerated using three typical tubular ports (Envicon). The total gas hold-up was determined by measuring the aerated and unaerated level difference, and the local gas hold-up in the downcomer by pressure difference measurements. An impeller anemometer was inserted between the edge of the module dummy and the tank bottom to determine the circulating liquid velocity.

### 2.2. Numerical methods

*Single bubbles.* The system was calculated with the VOF method in Fluent© using the material properties of water and air. Bubble size (3–10 mm), gap distance (3–7 mm) and, with regard to a loop reactor, the superimposed liquid velocity (0–60 cm/s) were varied. A grid for a single gap was set up with a height of 1200 mm to ensure that the bubble is able to reach its terminal rise velocity. Only one half of the channel and therefore also only one half of the bubble was simulated (see Fig. 2). In the centre between the two walls (membranes) a symmetry plane was set. Since the main bubble movement direction is upwards and parallel to the walls, this is a reasonable assumption. Depending on the gap distance, the bubble was initialised as a sphere or a cylinder, respectively, when the gap distance was smaller than the equivalent diameter of the spherical bubble. A moving mesh was used to ensure that the flow near the rising bubble is always well resolved without having a large number of cells that would lead to a very long calculation time. A User Defined Function was used to adjust the movement of the mesh to the movement of the bubble in every time step. Layering was used at the

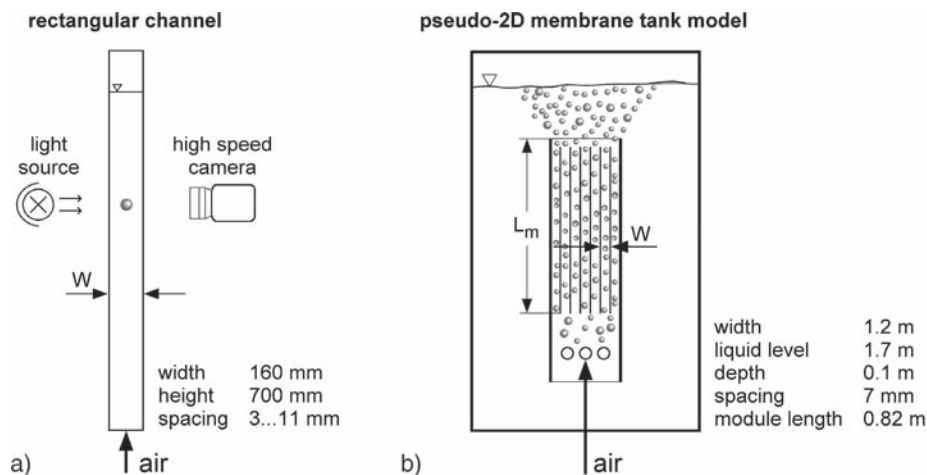


Fig. 1. Experimental set-up for (a) single bubble investigations and (b) the circulating tank flow.

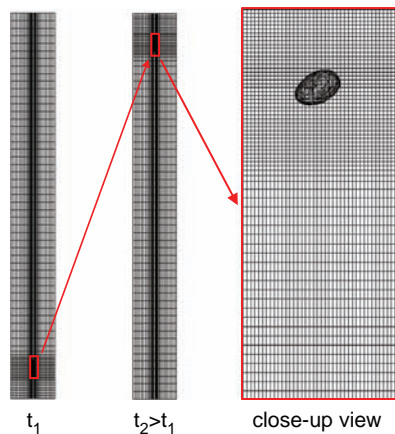


Fig. 2. Front view of the grid with different positions of the fine mesh around the bubble coupled with the vertical bubble movement.

top and the bottom of the mesh to collapse and split too small and too big cells. For the cases without superimposed liquid velocity, simulations were validated with experimental data (terminal rising velocity) and agreed within 5%.

*Tank flow.* The circulating multiphase flow was simulated with CFX-11 using an Eulerian–Eulerian approach and the Grace model to capture momentum transfer between the continuous (water) and dispersed phase (air). Turbulence was accounted for by using the shear

stress transport model for the continuous and the zero equation model for the dispersed phase. Steady state simulations were performed on a 2D mesh consisting of approx. 35,000 hexahedral cells. Instead of modelling the free liquid surface, a degassing boundary condition was used. A bubble size of 1.8 mm was applied which yielded gas hold-ups that were comparable with experimental observations.

### 3. Results

#### 3.1. Single bubble rise trials

The developed model allowed simulating the ascent of single bubbles up to a steady or rather periodic state. Calculating half a bubble as opposed to a quarter [17] enabled a periodic swinging motion parallel to walls (Fig. 3) which was in good agreement with experiments.

Figure 4 shows CFD results on the maximum wall shear stress exerted by rising bubbles in differently spaced channels. As expected, the highest shear rates are obtained in the smallest channels. An increase of bubble size above a certain diameter does not yield higher shear stress (although, to assess the shear force, the surface area on which this acts needs to be taken into account). Without superimposed liquid velocity, the shear stress seems to level off with increasing bubble size for each gap, and even drops to lower values for high liquid velocities. This is in agreement with Ndinisa et al. (2006) [11] who observed that as bubble size increases, so does the clean-

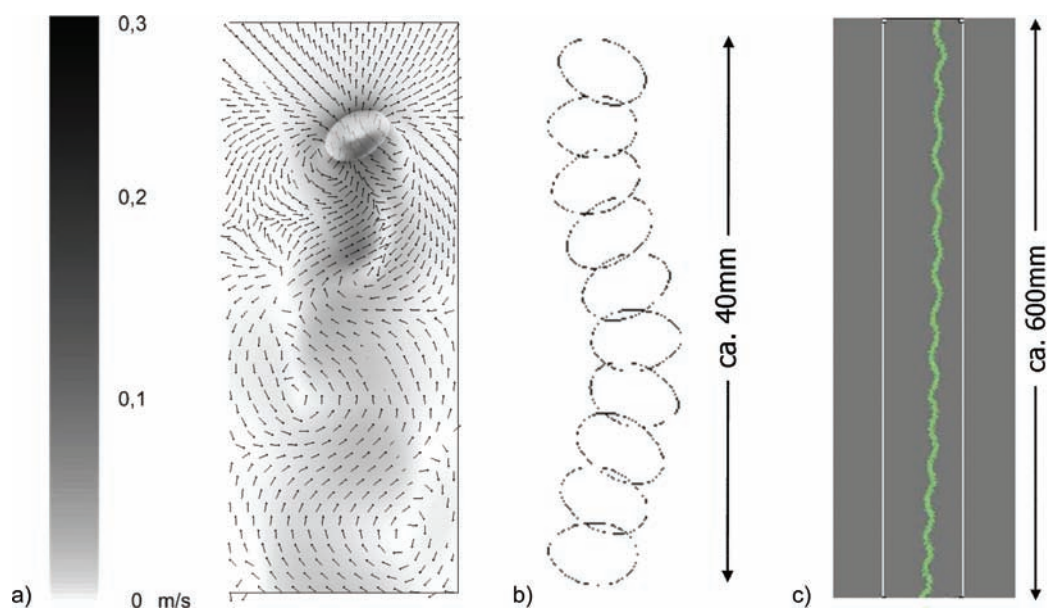


Fig. 3. 5 mm bubble, 5 mm gap, stagnant water: (a) velocity field near the bubble (simulation), (b) one period of the bubble movement (simulation), (c) rising path (experiment).

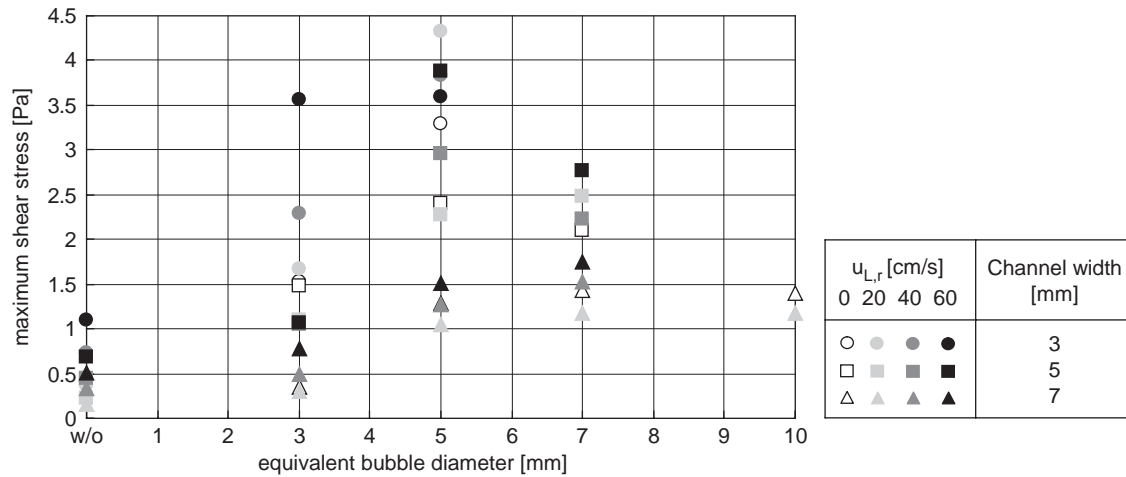


Fig. 4. CFD results for maximum wall shear stress exerted by differently sized bubbles rising at terminal rise velocity in channels of different widths.

ing effect, however, when bubbles became larger than the gap, a further increase in size only had a minor effect. With 0.7 Pa, the maximum shear stress found by Ndinisa et al. (2006) [15] at the highest air flow rate used was considerably smaller than the values shown in Fig. 4. However, since Ndinisa et al. (2006) [15] did not provide a downcomer region outside the module where any recirculating flow due to continuity happened within the module whereby the overall flow was slowed down. Fig. 4 also shows the impact of typical additional liquid crossflow velocities. For one bubble size/gap combination, an increasing superimposed liquid velocity does not ultimately lead to a rise in shear stress. In most cases the result is higher than the sum, which might be attributed to the lack of flow reversal in the liquid film when there is an overall upward motion. Sometimes, however, the total is considerably lower (e.g., 5 mm bubble in 3 mm gap with  $u_L = 60$  cm/s) which shows that in flat sheet applications matters are more complicated because the liquid can also plunge down on the unconfined sides of the bubble. Still, shear stress values achieved in two-phase flow are at least three times higher than those obtained by single-phase flow. In (membrane bioreactors or) real filtration systems, the fluids have other material properties than water and tend to clog the gaps between the membranes. Therefore, besides additional possible construction problems of small gaps, a gap wider than 3 mm is preferable. Thus, the highest shear stress values arise for a 5 mm bubble in a 5 mm gap with 60 cm/s superimposed liquid velocity.

### 3.2. Two-phase flow in the tank

For a systematic optimisation, a reliable model is needed. Several authors have tried to apply the well

known approach by Chisti et al. (1988) [20] to predict liquid velocities in submerged MBR modules [14,21]. Sofia et al. were quite successful, but in their set-up, only a single membrane plate was introduced so any resistance caused by the presence of the module was very small. Such additional resistance, however, would impact on the driving force for the liquid movement (difference in gas hold-ups and hence hydrostatic pressures between riser and downcomer) and on the flow itself due to the increased wall friction. Both aspects were taken into account by modifying the Chisti model accordingly [16,17] as described in the following. In contrast to the slender airlift reactors studied by Chisti et al., MBRs typically have significantly different width/height and riser/downcomer cross section area ratios. This, and the fact that the presence of the membranes alters the rise velocity, results in the necessity to modify the relationship between two central entities in the calculation, the gas hold-ups  $\epsilon$  in the downcomer  $d$  and in the riser  $r$ . According to [22], the riser gas hold-up can be estimated by

$$\epsilon_r = \frac{u_{G,r}}{0.24 + 1.35 \cdot (u_{G,r} + u_{L,r})^{0.93}} \quad (\text{with } u \text{ in m/s}) \quad (1)$$

This correlation was shown to be valid for MBRs [16,17]. In the downcomer, however, the observed gas hold-ups were significantly lower than the 89% of  $\epsilon_r$  reported by [23]. In contrast to this linear correlation used by [20], the following correlation was obtained

from measurements using different  $A_r/A_d$  ratios and superficial gas velocities [17]:

$$\epsilon_d = 0.016 \cdot \left( \frac{u_{L,r} \frac{A_r}{A_d}}{u_{B,s}} \right)^{1.48} \cdot \epsilon_r^{0.032} \quad (2)$$

The additional membrane wall friction was estimated with a corrective factor  $\Psi_{kf}$  acc. to [24] and the single phase friction factor  $K_M$  calculated using the Hagen-Poiseuille law for laminar or the Blasius equation for turbulent flow. The resulting modified Chisti equation is:

$$u_{L,r} = \left( \frac{2gh(\epsilon_r - \epsilon_d)}{K_b \left( \frac{A_r}{A_d} \right)^2 \frac{1}{(1 - \epsilon_d)^2} + \Psi_{kf} K_M \frac{1}{2} \left( \frac{A_r}{A_M} \right)^2 \frac{L_M (W + T)}{W \cdot T}} \right)^{0.5} \quad (3)$$

which together with eqns. (1) and (2) give the full iterative model. Both superficial velocities are defined with the empty riser cross section area. Fig. 5 shows that the model prediction fits well but slightly exceeds experimental data. This can be attributed to the fact that the decelerating effect of the aeration tubes used in the experimental set-up has not yet been included in the model. The CFD results shown are based on simulations with 1.8 mm bubbles which gave gas hold-ups close to the ones that were observed in experiments. However, due to simplifying assumptions like monodispersity and incompressibility which were made to reduce the numerical effort, superficial liquid velocities are still somewhat overestimated. Fig. 5 also shows that the increase of achieved liquid velocities tends to become less. In other words, exceeding a certain gas flow rate does not yield much additional effect. Average gas velocity in the module gaps ( $u_{G,g} = \dot{V}_{air}/A_{gaps}$ ) was

found to vary between 0.04 and 0.1 m/s across a number of modern large pilot and full-scale plants [3]. Assuming a typical gap/riser cross section ratio of around 0.5, this translates to  $u_{G,r} \approx 0.02 \dots 0.05$  m/s, i.e., in some cases it might be in the region where it does not significantly impact on the liquid circulation velocity.

The abrupt flow direction change from the down-comer to the riser region causes significant frictional losses. Thus a smoother draft tube edge was introduced to achieve lower bend loss and thus higher circulation velocities (see Fig. 6) [17]. An additional acceleration was achieved by locating the aerators at the bottom of the tank instead of at the entrance to the draft tube where they block the available cross section and slow down the flow. Together with spargers inside the flow bodies, also a much more homogenous bubble distribution across the whole module could thus be achieved which prevents clogging of the outer channels. With this configuration, either higher shear forces can be achieved at the same aeration or significantly lower aeration is required to achieve the same liquid velocity.

#### 4. Conclusions

To achieve a more efficient deposition control on flat sheet membranes in MBRs, different aspects of the hydrodynamic design were studied in this work. Investigations on single bubbles were carried out to determine the optimal values for the membrane distance, bubble size and superimposed liquid velocity with the maximum shear stress as the objective function. For the system air/water the highest shear stress was found for a 5 mm bubble in a 5 mm gap with 60 cm/s superimposed liquid velocity. A moving grid, coupled with the rising bubble was applied to enable highly resolved simulations with reasonable effort. A second aspect was the relation between the aeration rate and the circulation

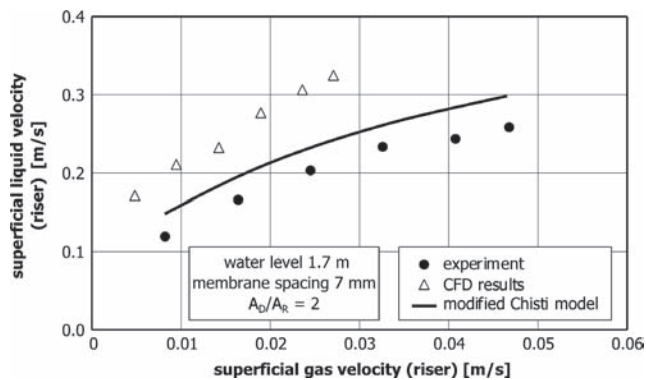


Fig. 5. Superficial liquid velocities achieved using different gas flow rates: exp. and num. results in comparison with the modified model acc. to Chisti et al. (1988) [20].

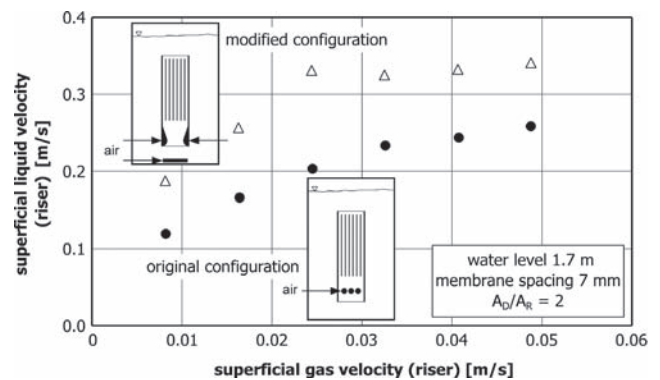


Fig. 6. Circulating velocities achieved by conventional and modified aerator configuration.

velocity in MBR which can be improved by optimising MBR tank, sparger and module geometries. A modification of the Chisti model for airlift loop reactors was presented which can be used as a design rule for tank and module geometry or aeration rate. At the same gas flow rate, a 30–50 % increase in liquid circulating velocity was achieved by a simple modification of the sparger and the entry zone to the riser section.

### Acknowledgements

We thank the Deutsche Bundesstiftung Umwelt DBU (German Foundation for the Environment) for financial support to parts of this work.

### Nomenclature

$A_{b,r}$ , m <sup>2</sup>	free area for flow between riser and downcomer
$A_{d,r}$ , m <sup>2</sup>	cross-sectional area of the downcomer
$A_{M,r}$ , m <sup>2</sup>	free area for flow between the membrane plates
$A_{r,r}$ , m <sup>2</sup>	cross-sectional area of the riser
$K_b$	resistance coefficient of the flow direction turn at the bottom
$K_M$	resistance coefficient of the membrane module
$g$ , m/s <sup>2</sup>	gravitational constant
$h$ , m	gas-liquid dispersion height
$L_{M,r}$ , m	height of the membrane module
$T$ , m	depth of the membrane module
$u_{g,r}$ , m/s	superficial gas velocity (riser)
$u_{l,r}$ , m/s	superficial liquid velocity (riser)
$u_{B,s}$ , m/s	rising velocity for the maximum stable bubble diameter
$W$ , m	distance between the membrane plates

### Greek Symbols

$\epsilon_d$	gas holdup (downcomer)
$\epsilon_r$	gas holdup (riser)
$\Psi_{Kf}$	(two phase flow) corrective factor

### References

- [1] S. Judd, The MBR Book, Elsevier, Amsterdam (2006).
- [2] H. Fletcher, T. Mackley and S. Judd, The cost of a package plant membrane bioreactor, *Water Res.* 41 (2007) 2627–2635.
- [3] B. Verrecht, S. Judd, G. Guglielmi, C. Brepols and J.W. Mulder, An aeration energy model for an immersed membrane bioreactor, *Water Res.*, 42 (2008) 4761–4770.
- [4] Z.F. Cui, S. Chang and A.G. Fane, The use of gas bubbling to enhance membrane processes, *J. Membr. Sci.*, 221 (2003) 1–35.
- [5] T. Taha and Z.F. Cui, Hydrodynamic analysis of upward slug flow in tubular membranes, *Desalination*, 145 (2002) 179–182.
- [6] A.G. Fane, A. Yeo, A. Law, K. Parameshwaran, F. Wicaksana and V. Chen, Low pressure membrane processes – doing more with less energy, *Desalination*, 185 (2005) 159–165.
- [7] E. Germain, T. Stephenson and P. Pearce, Biomass characteristics and membrane aeration: Toward a better understanding of membrane fouling in submerged membrane bioreactors (MBRs), *Biotech. Bioeng.*, 90 (2005) 316–322.
- [8] A.P.S. Yeo, A.W.K. Law and A.G. Fane, The relationship between performance of submerged hollow fibers and bubble-induced phenomena examined by particle image velocimetry, *J. Membr. Sci.*, 304 (2007) 125–137.
- [9] G. Ducom, F.P. Puech and C. Cabassud, Air sparging with flat sheet nanofiltration: a link between wall shear stresses and flux enhancement, *Desalination*, 145 (2002) 97–102.
- [10] K. Essemiani, G. Ducom, C. Cabassud and A. Liné, Spherical cap bubbles in a flat sheet nanofiltration module: experiments and numerical simulation, *Chem. Eng. Sci.*, 56 (2001) 6321–6327.
- [11] N.V. Ndinisa, A.G. Fane and D.E. Wiley, Fouling control in a submerged flat sheet membrane system: Part I - bubbling and hydrodynamic effects, *Sep. Purif. Technol.*, 41 (2006a) 1383–1409.
- [12] H. Nagaoka, A. Tanaka and Y. Toriizuka, Measurement of effective shear stress working on flat sheet membrane by air scrubbing, *Water Supply*, 3(5) (2003) 423–428.
- [13] G. Ducom, F.P. Puech and C. Cabassud, Gas/Liquid two-phase flow in a flat sheet filtration module: measurement of local wall shear stresses, *Can. J. Chem. Eng.*, 81 (2003) 771–775.
- [14] A. Sofia, W.J. Ng and S.L. Ong, Engineering design approaches for minimum fouling in submerged MBR, *Desalination*, 160 (2004) 67–74.
- [15] N.V. Ndinisa, A.G. Fane, D.E. Wiley and D.F. Fletcher, Fouling control in a submerged flat sheet membrane system: part II – two-phase flow characterization and CFD simulations, *Sep. Sci. Technol.*, 41 (2006b) 1411–1445.
- [16] H. Prieske, A. Drews and M. Kraume, Prediction of the circulation velocity in a membrane bioreactor, *Desalination*, 231 (2008) 219–226.
- [17] A. Drews, H. Prieske and M. Kraume, Optimierung der Blasen- und Zirkulationsströmung in Membranbelebungsreaktoren, *Chem. Ing. Tech.*, 80(12) (2008a) 1795–1801.
- [18] A. Drews, H. Prieske, E.-L. Meyer, G. Senger and M. Kraume, Advantageous and detrimental effects of air-sparging in membrane filtration: bubble movement, exerted shear and particle classification, In 12th AMK, Aachen 2008b.
- [19] K. Zhang, Z. Cui and R.W. Field, Effect of bubble size and frequency on mass transfer in flat sheet MBR, *J. Membr. Sci.*, 332 (2009) 30–37.
- [20] M.-Y. Chisti, B. Halard and M. Moo-Young, Liquid circulation in airlift reactors, *Chem. Eng. Sci.*, 43(3) (1988) 451–457.
- [21] E. McAdam, S.J. Judd, R. Gildemeister, A. Drews and M. Kraume, Critical analysis of submerged membrane sequencing batch reactor operating conditions, *Water Res.*, 39 (2005) 4011–4019.
- [22] J.H. Hills, The operation of a bubble column at high throughputs. I. Gas holdup measurement, *Chem. Eng. J.*, 12 (1976) 89–99.
- [23] R.A. Bello, C.W. Robinson and M. Moo-Young, Gas Holdup and overall volumetric oxygen transfer coefficient in airlift contactors, *Biotechnol. Bioeng.*, 27(3) (1985) 369–381.
- [24] R.W. Lockhart and R.C. Martinelli, Proposed Correlation of data for isothermal two-phase, two-component flow in pipes, *Chem. Eng. Progr.*, 45 (1949) 38–48.